Transp Porous Med (2013) 97:135–145
DOI 10.1007/s11242-012-0112-z

Analytic Model for DBF Under Multiple Particle Retention Mechanisms

Juliana Aragão Araújo · Adriano Santos

Received: 4 June 2012 / Accepted: 17 December 2012 / Published online: 1 January 2013

Abstract Discrepancies between classical model (CM) predictions and experimental data for deep bed filtration (DBF) have been reported by various authors. In order to understand these discrepancies, an analytic continuum model for DBF is proposed. In this model, a filter coefficient is attributed to each distinct retention mechanism (straining, diffusion, gravity interception, etc.). It was shown that these coefficients generally cannot be merged into an effective filter coefficient, as considered in the CM. Furthermore, the derived analytic solutions for the proposed model (PM) were applied for fitting experimental data, and a very good agreement between experimental data and PM predictions were obtained. Comparison of the obtained results with empirical correlations allowed identifying the dominant retention mechanisms. In addition, it was shown that the larger the ratio of particle to pore sizes, the more intensive the straining mechanism and the larger the discrepancies between experimental data and CM predictions. Finally, the CM and PM were compared via statistical analysis. The obtained p values allow concluding that the PM should be preferred especially when straining plays an important role.

Keywords Deep bed filtration · Retention mechanisms · Straining · Attachment · Analytic modeling

1 Introduction

Owing to its scientific and industrial importance, modeling of deep bed filtration (DBF) in porous media has been intensively studied in the recent years (Herzig et al. 1970; Tien and Ramarao 1995; Elimelech et al. 1995). During waterflooding in oil reservoirs, for example, suspended particles can plug pores causing formation damage and permeability decline. Predicting the influence of different particle retention mechanisms on retention profile is

J. A. Araújo · A. Santos (✉)
Departamento de Engenharia de Petróleo, Universidade Federal do Rio Grande do Norte,
Av. Salgado Filho 3000, Natal, RN 59078-970, Brazil
e-mail: adriano@eq.ufrn.br

essential for understanding injectivity decline. During DBF, particles are retained in porous media by mechanisms like straining and attachment (Elimelech et al. 1995; Israelachvili 2007; Sharma and Yortsos 1987). The effectiveness of each particle retention mechanism depends on the suspended particle's concentration, particle and pore size distributions, particle–pore and particle–particle interactions, composition of the suspensions, velocity, etc.

Straining occurs when a pore throat is reached by a suspended particle larger than itself. On the other hand, small particles can be retained because of diffusion, and electric and gravitational forces. In this case, particles are retained because they are deviated (toward pore walls) from the trajectory suggested by flow-lines.

In the classical model (CM) (Iwasaki 1937; Herzig et al. 1970; Tien and Ramarao 1995), all retention mechanisms are represented by a unique "effective filtration coefficient," which is assumed to be equal to the summation of filter coefficients related to each operative retention mechanism. The CM and its analytic solutions have been widely applied for studying DBF. However, significant discrepancies between the experimental data and the CM predictions have been reported by various authors (Bradford et al. 2002, 2003; Bradford and Bettahar 2006; Tufenkji et al. 2004). These discrepancies have been attributed to grain surface roughness (Bradford et al. 2002; Redman et al. 2001) and charge heterogeneity across the porous medium (Bradford et al. 2004). Furthermore, some discrepancies between the theory and experimental data may also be because CM does not take straining into account (Bradford et al. 2002).

Recently, Santos and Barros (2010) proposed a *discrete* micro model taking multiple particle retention mechanisms into account. Their model showed a very good agreement with the studied experimental data and allowed explaining discrepancies observed in CM predictions. However, the above mentioned model can be applied if, and only if, filter coefficients are constant.

In this article, a *continuum* scale model for DBF under multiple particle retention mechanisms is proposed. Contrary to the Santos and Barros (2010) model, the *continuum* proposed model (PM) allows considering variable filter coefficients.

The CM and PM parameters were determined by fitting experimental data available in the literature. Comparison of the results allowed concluding that the PM showed a significantly better agreement with the studied experimental data. In addition, the obtained filter coefficients were compared to those obtained by means of empirical correlations available in the literature, and a good agreement was observed.

2 Analytic Model for DBF

In this section, the PM for DBF is discussed, and analytic solutions are derived. The PM was developed considering incompressible flow in a porous media with constant porosity (φ). In addition, DBF occurs if, and only if, retention probabilities tend to zero (Santos and Barros 2010). Therefore, the probability of a particle to be simultaneously captured by two or more mechanisms can be neglected, and DBF of each particle population (subjected to a specific retention mechanism) is governed by the following equations:

$$\begin{cases} \dfrac{\partial c_i}{\partial T} + \dfrac{\partial c_i}{\partial X} = -\dfrac{\partial \sigma_i}{\partial T} \\ \dfrac{\partial \sigma_i}{\partial T} = \lambda_i L c_i \end{cases} \tag{1}$$

where

$$X = \frac{x}{L} \quad \text{and} \quad T = \frac{1}{L\varphi} \int_0^t U\left(t'\right) \mathrm{d}t' \tag{2}$$

In the above equations, $U(t)$ is the Darcy velocity (volumetric flow rate per unit of area), and L is the porous media length. In addition, σ_i is the particle concentration retained because of the ith mechanism, c_i represents the suspended particle concentration subjected to the ith mechanism, and λ_i is the filter coefficient (retention probability per unit of length) due to the ith mechanism.

Assuming that initially there are no particles in porous medium and that the injected particle concentration subjected to the ith mechanism ($c_{0,i}$) is constant, it follows that

$$\begin{cases} T = 0;\, c_i\,(X, 0) = \sigma_i\,(X, 0) = 0 \\ X = 0;\, c_i\,(0, T) = c_{0,i} \end{cases} \tag{3}$$

Owing to changes on porous media retention efficiency, the filter coefficients (λ_i) are generally functions of retained particle concentrations $\lambda_i = \lambda_i(\sigma_1, \sigma_2, \ldots, \sigma_n)$.

The model (1–3) tends to CM if, and only if, a single mechanism is operative. However, the CM has been widely applied in cases where multiple particle retention mechanisms are operative. In this case, it is assumed that an *effective* filtration coefficient equals the summation of all individual filter coefficients, i.e., $\lambda = \Sigma\lambda_i$. Many authors (Herzig et al. 1970; Maroudas 1961; Maroudas and Eisenklam 1965; Maroudas 1966; Ives and Pienvichitr 1965; Alvarez 2004) have proposed analytic solutions for the CM assuming a variety of effective filtration coefficients. Unfortunately, significant discrepancies between experimental data and CM predictions have been reported in the literature (Bradford et al. 2003; Tufenkji and Elimelech 2004; Santos and Barros 2010).

It is important to highlight that if $\lambda_i = \lambda_i(\sigma_i)$, then the system (1) can be solved independently for the ith particle populations (c_i and σ_i). In this case, the classical analytic solutions can be rewritten to obtain analytic solutions for a specific retention mechanism.

During transport of monosized particles in porous media, straining and deposition (gravity, interception, diffusion, etc.) occur in pores smaller and larger than the particle size, respectively. Considering that deposition in large pores results in a linear filter coefficient function

$$\lambda_i\,(\sigma_i) = \lambda_{0,i} - b_i\sigma_i \tag{4}$$

The analytic solution for the Eq. (1), subjected to the initial and boundary conditions (3), is given by

$$c_i\,(X, T) = \begin{cases} \dfrac{c_{0,i}}{1 + \exp\left[-b_i L c_{0,i}\,(T - X)\right]\left[\exp\left(\lambda_{0,i} L X\right) - 1\right]}, & X \le T \\ 0, & X > T \end{cases} \tag{5}$$

$$\sigma_i\,(X, T) = \begin{cases} \dfrac{\lambda_{0,i}}{b_i}\left[1 + \dfrac{\exp[\lambda_{0,i} L X]}{\exp(b_i L c_{0,i}(T - X)) - 1}\right]^{-1}, & X \le T \\ 0, & X > T \end{cases} \tag{6}$$

where $\lambda_{0,i}$ (the initial filter coefficient) and b_i are constants. In addition, particle retention can cause favorable ($b_i < 0$) or unfavorable ($b_i > 0$) interactions for further deposition.

In Appendix, it is shown that, during DBF of monosized particles, the filter coefficient for straining mechanism is a decreasing function of the retained particle concentration (see

Appendix, Eq. (24)). Moreover, it is shown that the filter coefficient can be approximated by a linearly decreasing function of retained particle concentration (see Eq. (28)). Finally, if the concentration of pores smaller than the injected particle is much larger than the concentration of particles retained by straining, then the filter coefficient related to straining can be considered constant (see Eq. (28)). In this case, when b_i tends to zero in Eqs. (5) and (6), it follows that

$$c_i(X,T) = \begin{cases} c_{0,i}\, e^{-\lambda_{0,i} L X}, & X \le T \\ 0, & X > T \end{cases} \tag{7}$$

$$\sigma_i(X,T) = \begin{cases} \lambda_{0,i} L c_{0,i} (T - X)\, e^{-\lambda_{0,i} L X}, & X \le T \\ 0, & X > T \end{cases} \tag{8}$$

If n distinct retention mechanisms are operative, then the global suspended and retained particle concentrations (c and σ, respectively) can be obtained by adding the populations' concentrations as follows:

$$c(X,T) = \frac{\sum_{i=1}^{n} c_i(X,T)}{\sum_{i=1}^{n} \alpha_i} \tag{9}$$

$$\sigma(X,T) = \frac{\sum_{i=1}^{n} \sigma_i(X,T)}{\sum_{i=1}^{n} \alpha_i} \tag{10}$$

where α_i is the fraction of injected particle concentration subjected to the ith mechanism.

Considering that a fraction "α_1" ($\alpha_1 = c_{0,1}/c_0$) of injected particles is subjected only to straining (mechanism 1) and a fraction "α_2" ($\alpha_2 = c_{0,2}/c_0$) of injected particles is subjected only to deposition (mechanism 2), it follows that $\alpha_1 + \alpha_2 = 1$. Finally, substitution of Eqs. (5–8) into Eqs. (9) and (10) allows obtaining analytic solutions for global concentrations c and σ.

3 Experimental Section

In this section, the experiments conducted by Bradford et al. (2002) are briefly discussed. In these experiments, fluorescent monosized latex particles were injected in a variety of porous media. The injected particle concentration was particle size dependent; for particles 0.45, 1, and 3.2 μm, the injected concentrations were 4.24×10^{11}, 3.86×10^{10}, and 1.18×10^{9} particles/l, respectively. These concentrations were selected to minimize any permeability reduction.

The porous media consist of Ottawa sand packs with a variety of grain sizes. The porous media were named 2030, 3550, MIX, and 70110 with medium grain sizes of 0.71, 0.36, 0.15, and 0.24 mm, respectively. Ottawa sands consisting of 99.8 % SiO_2 (quartz) and trace amounts of metal oxides are spheroidal in shape, and may have rough surfaces. The soil columns were 15 cm in length and 4.8 cm in diameter. In addition, Bradford and Abriola (2001) reported that 2, 6.5, 16, and 30 % of the pore spaces contain pores less than 10 μm in diameter for the 2030, 3550, MIX, and 70110 sands, respectively. In contrast, glass beads (GBs) are relatively chemically homogeneous, spherical, and smooth with an average grain diameter of 0.26 mm.

Before suspensions injection, porous media were flushed with several pore volumes (PVs) of eluant solution to remove natural colloids particles from the porous media.

During suspension injection, samples were gathered during each 5-min time interval and then capped. The effluent colloid concentration (c_{eff}) was then determined on these samples,

and the results are shown in Figs. 1a and 3a. Following completion of the colloid transport experiments, the spatial distribution of colloids in a soil column was determined (see Figs. 1b, 2, 3b, 4).

4 Results and Discussion

In this section, the experimental data presented by Bradford et al. (2002) were fitted considering both the PM and CM. The models parameters, see Table 1, were obtained by least squares method.

Based on Bradford et al. (2003), we assumed that straining was the dominant mechanism especially for large particles (3.2 μm). Therefore, the filter coefficient $\lambda_{0,1}$ (which is always significantly larger than $\lambda_{0,2}$, see Table 1), is attributed to the straining mechanism. In addition, considering a constant filter coefficient for straining, a very good agreement between experimental data and the PM predictions was verified (see Figs. 1, 2, 3, 4). It suggests that, in the studied experiments, the concentration of pores smaller than the injected particles is much larger than the retained particle concentration (see Eq. 28).

In addition, notice that $\lambda_{0,2}$ has the same order of magnitude of empirical correlations proposed by Tufenkji and Elimelech (2004) and Yao et al. (1971); see Table 1. These correlations were obtained from experiments where straining was not operative. Therefore, λ_2 is attributed to other mechanisms (diffusion, interception, and gravity).

It is important to highlight that the larger the particle size, the larger the filter coefficient ($\lambda_{0,1}$) and the larger the fraction of particles subjected to straining (α_1), see Table 1. Notice that straining was very intensive ($\lambda_{0,1} \gg \lambda_{0,2}$) in all the studied cases. Furthermore, Table 1shows the mean squared error (Draper and Smith 1967) for the PMs and CMs (MSEp and $\mathrm{MSE_{CL}}$, respectively). Notice that MSEp valus are significantly smaller than those of $\mathrm{MSE_{CL}}$, especially for large particles (3.2 μm), where straining was the dominant particle retention mechanism. Finally, the PM and CM were compared using an F test (Draper and Smith 1967). Comparison of the obtained p values (see Table 1) allows concluding that the larger the particle size, the more intensive is the straining mechanism and the more appropriate is the PM when compared with the CM predictions. Therefore, the PM should be preferred especially when straining plays an important role.

It is also important to highlight that pores are smaller in porous media 3550 (medium grain size equals 0.36 mm) than in porous media 2030 (medium grain size equals 0.71 mm). The obtained results for these porous media suggest that the larger the amount of small pores, the larger the fraction of particles subjected to straining (α_1) and the more intensive is the straining mechanism (i.e., larger $\lambda_{0,1}$, see Table 1 and Eq. (25)).

The CM (constant filtration coefficient) and the PM predictions are shown in Figs. 1, 2, 3, and 4. Figure 1a shows that CM and PM predictions for effluent concentration (c_{eff}) are very similar only for large particles (3.2 μm). However, notice that 3.2 μm retained particle concentrations predicted by CM significantly deviate from the studied experimental data (see Fig. 1b). On the other hand, the PM showed a good agreement with the experimental data for both effluent and retained concentrations (see Figs. 1, 2). In addition, Figs. 1b and 2 show that the larger the particle size, the more intensive is the particle retention that occurred near to the porous media entrance. Bradford and Abriola (2001) suggested this occurred because straining was the dominant mechanism in the experiments they conducted.

Figure 3a shows the CM and the PM predictions for effluent concentration (c_{eff}). Green line represents CM prediction considering constant filtration coefficient (CM*cfc*). However, because c_{eff} is a monotonically increasing function in this case, a monotonically decreasing

Table 1 PM parameters: α_1, $\lambda_{0,1}$, $\lambda_{0,2}$, and b_2; classical filtration coefficient (λ_{CL}); and filtration coefficients obtained by using Tufenkji & Elimelech (λ_{TE}) and Yao & Habibian (λ_{YH}) empirical correlations

Porous media	d_p (μm)	α_1 (%)	$\lambda_{0,1}$ (m^{-1})	$\lambda_{0,2}$ (m^{-1})	b_2 (mm^{-1})	λ_{CL} (m^{-1})	λ_{TE} (m^{-1})	λ_{YH} (m^{-1})	MSE_P ($\times 10^{-3}$)	MSE_{CL} ($\times 10^{-3}$)	p value
2030	0.45	0.006	20.31	1.61	23.3	1.16	1.10	1.41	2.50	2.16	0.66
	1	0.003	26.89	1.18	0.32	1.18	1.10	1.55	56.0	48.0	1.00
	3.2	4.1	166.9	7.22	0.31	7.50	4.44	7.01	192	189	0.74
3550	0.45	4.2	51.72	2.12	25.88	1.88	1.48	1.93	2.26	5.84	3.92×10^{-4}
	1	2.7	63.08	1.88	26.30	1.55	0.89	1.26	3.50	4.71	25×10^{-3}
	3.2	40.9	176.7	5.68	13.14	9.28	7.17	11.43	139.0	1532.0	8.32×10^{-7}
Mix	0.45	1.0	92.4	1.92	22.9	1.47	0.76	0.99	4.06	5.04	0.057
	1	2.0	96.6	2.40	24.22	1.87	13.2	18.4	2.58	3.21	0.04
	3.2	67.0	99.7	11.61	19.53	19.95	15.98	24.8	733.0	2990.0	2.61×10^{-5}
70110	0.45	8.4	69.65	4.65	34.15	3.84	3.06	4.05	7.93	50.0	1.85×10^{-6}
	1	28.6	75.89	6.05	38.23	6.90	5.40	7.481	9.72	133.0	1.17×10^{-6}
	3.2	44.6	480.0	21.28	0.64	25.76	39.57	62.04	140.0	1305.0	2.77×10^{-7}
GB	0.45	21.3	111.5	2.27	0.5	4.65	3.06	4.072	619.0	1984.0	8.49×10^{-4}
	1	46.9	113.1	13.11	0.07	19.4	13.85	19.71	274.0	2458.0	6.49×10^{-7}
	3.2	86.5	178.9	20.01	0.51	40	50.38	80.32	312.0	16189.0	2.35×10^{-12}

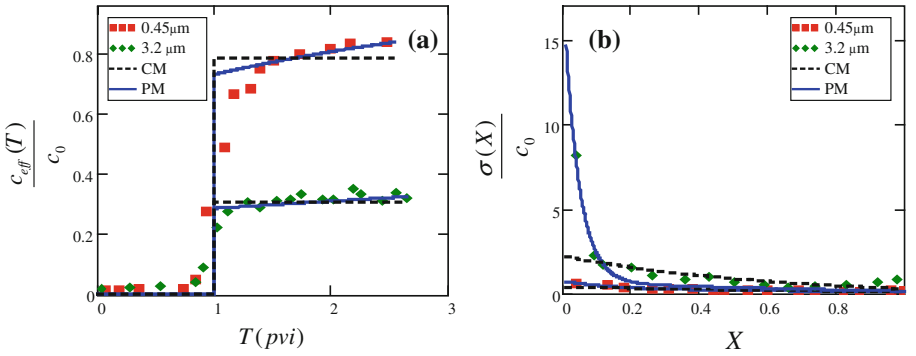

Fig. 1 Experimental data and modeling for injection of colloids (0.45 and 3.2 µm diameters) across porous media 3550: **a** Breakthrough curves and **b** retained particle profile

Fig. 2 Retained particle profile for injection of colloids (sizes 0.45 and 3.2 µm) across porous media 70110

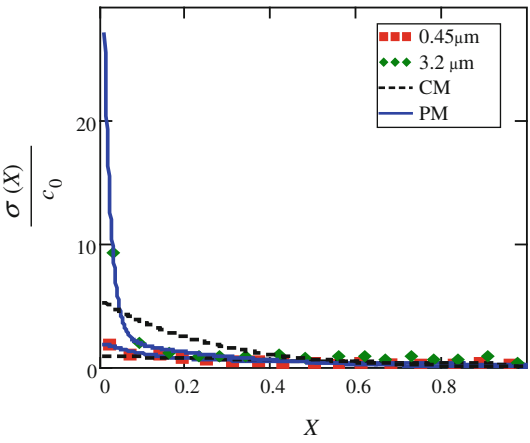

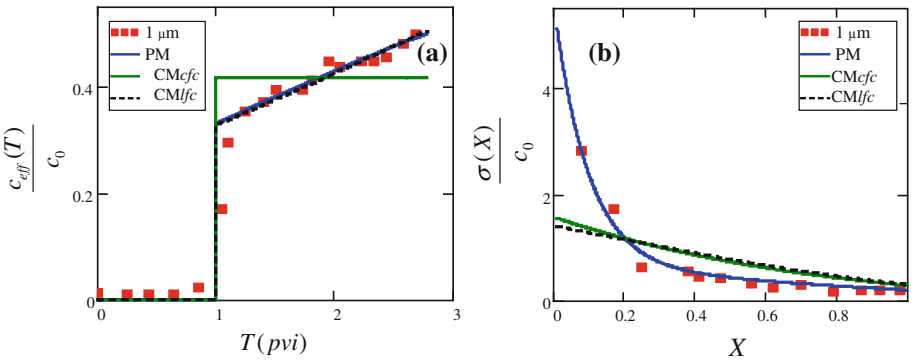

Fig. 3 Experimental data and modeling for injection of colloids (1.0 µm diameter) across porous media 70110: **a** breakthrough curve; **b** spatial distribution of retained particles

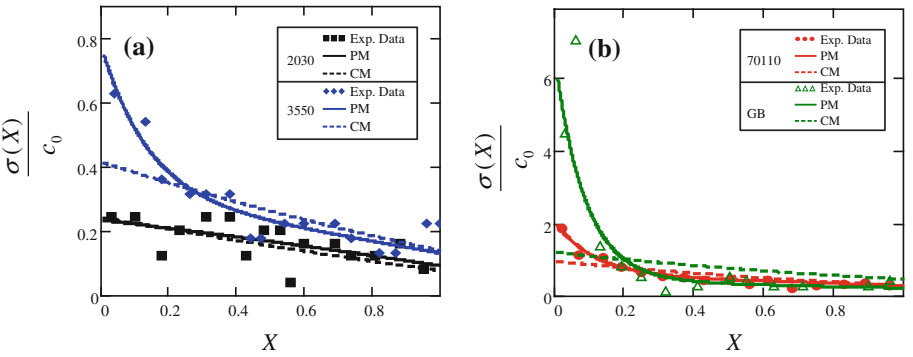

Fig. 4 Spatial distribution of retained 0.45 μm colloids

filtration function (e.g., $\lambda(\sigma) = \lambda_{CL} - b\sigma$) is more appropriate (Tien and Ramarao 1995). Dashed black line in Fig. 3a represents the CM fitting considering linear decreasing filtration coefficient function (CM*lfc*). Furthermore, blue line represents the PM fitting. The CM*lfc* showed a good agreement with the experimental data for effluent concentration (see Fig. 3a). However, a significant discrepancy between experimental data and CM prediction (CM*lfc*) for particle retention was noticed (see Fig. 3b). On the other hand, the PM predictions for both effluent and retained particle concentrations are in good agreement with the experimental data (see Fig. 3).

Figure 4 shows spatial distribution (experimental data and model predictions) of retained colloids in various porous media (2030, 3550, 70110 and GB). It is important to highlight that CM and PM predictions for retention of 0.45 μm into porous media 2030 and 3550 are very similar. In addition, notice that the smaller the pore size, the more intensive is the retention occurring near to the porous media entrance. It suggests that the smaller the ratio of pore to particle size, the more intensive the straining mechanism.

A very good agreement between experimental data and PM predictions was obtained (see Figs. 1, 2, 3, 4). Furthermore, the obtained results allowed interpreting experimental data and identifying the operative retention mechanisms (straining, interception, gravity, and diffusion). In general, the larger the ratio of the particle to pore sizes, the more intensive the straining mechanism and the larger the discrepancies between experimental data and CM predictions (see Figs. 1b, 2, 3b, 4). Therefore, the PM should be preferred especially when straining plays an important role (see *p* values in Table 1).

Acknowledgements The authors gratefully acknowlege the financial support provided by Petrobras (T.C. 0050.0022723.06.4). J. A. Araújo acknowledges the PhD scholarship provided by ANP/PRH 14.

Appendix: Filter Coefficient for Straining

In this section, we derive a filter coefficient function related to straining based on the following stochastic model for particle retention and pore blocking kinetics (Sharma and Yortsos 1987; Santos and Bedrikovetsky 2006; Santos et al. 2008), respectively:

$$\frac{\partial S}{\partial t} = \frac{1}{\Delta} \frac{\int_0^{r_s} r_p^4 H \mathrm{d}r_p}{\int_0^{\infty} r_p^4 H \mathrm{d}r_p} UC \tag{11}$$

$$\frac{\partial H}{\partial t} = -\frac{1}{\Delta}\frac{r_{\mathrm{p}}^4 H}{\int_0^\infty r_{\mathrm{p}}^4 H \mathrm{d}r_{\mathrm{p}}} U \int_{r_{\mathrm{p}}}^{\infty} C \mathrm{d}r \tag{12}$$

where H and C represent pore radius (r_{p}) and particle radius (r_{s}) concentration distributions, respectively. In addition, U is the Darcy's velocity, and Δ is the distance between subsequent pore throats. In Eq. (11), $\left(\int_0^{r_{\mathrm{s}}} r_{\mathrm{p}}^4 H \mathrm{d}r_{\mathrm{p}}\right)\left(\int_0^\infty r_{\mathrm{p}}^4 H \mathrm{d}r_{\mathrm{p}}\right)^{-1}$ represents the flow fraction through pores smaller than the particle size r_{s}. Therefore, the above mentioned fraction represents the retention probability for particles with size r_{s}.

Assuming that there are no suspended or deposited particles in the porous medium before the injection, we obtain the following initial and boundary conditions for the Eqs. (11) and (12):

$$\begin{array}{l} T = 0 : C = 0; \quad S = 0; \quad H = H_0 \\ X = 0 : C = C_0 \end{array} \tag{13}$$

where H_0 is the initial pore concentration distribution, and C_0 is the injected particle concentration distribution.

Let us consider transport of monosized particles:

$$C\left(r, x, t\right) = c\left(x, t\right)\delta\left(r - r_{\mathrm{s}}\right) \tag{14}$$

through a porous media with N distinct pore sizes:

$$H\left(r_{\mathrm{p}}, x, t\right) = h_1\left(x, t\right)\delta\left(r_{\mathrm{p}} - r_{\mathrm{p1}}\right) + \cdots + h_N\left(x, t\right)\delta\left(r_{\mathrm{p}} - r_{\mathrm{p}N}\right) \tag{15}$$

where h_i is the concentration of pores with radius $r_{\mathrm{p}i}$, and δ is the Dirac's delta function (see Fig. 5). In this case, substituting Eqs. (14) and (15) into Eqs. (11) and (12) results in

$$\frac{\partial \sigma}{\partial t} = \frac{1}{\Delta}\frac{\sum_{i=1}^{n} r_{\mathrm{p},i}^4 h_i}{\sum_{i=1}^{N} r_{\mathrm{p},i}^4 h_i} U c \tag{16}$$

$$\frac{\partial h_i}{\partial t} = \begin{cases} -\frac{1}{\Delta}\frac{h_i r_{\mathrm{p}i}^4}{\sum_{i=1}^{N} h_i r_{\mathrm{p}i}^4} U c, & i \le n \\ 0, & i > n \end{cases} \tag{17}$$

where n defines the largest pore radius ($r_{\mathrm{p}n}$) smaller than the particle radius (r_{s}), see Fig. 5. In addition, c and σ represent the suspended and retained particle concentrations, respectively.

Comparing the traditional particle retention kinetics (second equation in system (1)) with the Eq. (16), we obtain

$$\lambda = \frac{\sum_{i=1}^{n} h_i r_{\mathrm{p}i}^4}{\sum_{i=1}^{N} h_i r_{\mathrm{p}i}^4}\frac{1}{\Delta} \tag{18}$$

In addition, from Eq. (17), it follows that

$$\frac{\partial h_i}{\partial h_1} = \begin{cases} -\frac{r_{\mathrm{p}i}^4 h_i}{r_{\mathrm{p}1}^4 h_1}, & i \le n \\ 0, & i > n \end{cases} \tag{19}$$

The solution of Eq. (19) is given by

$$h_i\left(h_1\right) = \begin{cases} h_{i,0}\left(\frac{h_1}{h_{i,0}}\right)^{\left(r_{\mathrm{p}i}/r_{\mathrm{p}1}\right)^4}, & i \le n \\ h_{i,0}, & i > n \end{cases} \tag{20}$$

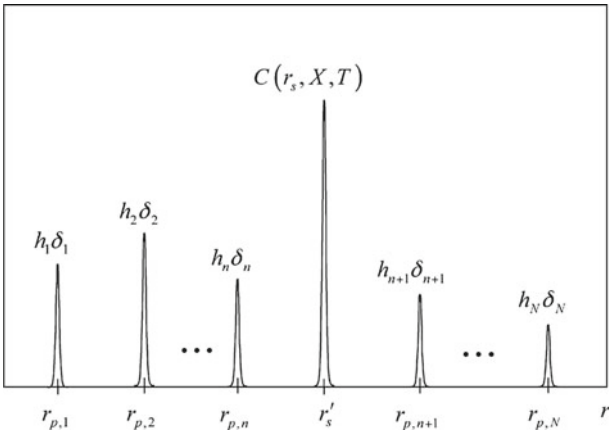

Fig. 5 Particle and pore concentration distributions

Moreover, the process of applying summation over all "i" in Eq. (20) and comparing the resulting equation with the Eq. (16) results in

$$\frac{\partial}{\partial t}\sum_{i=1}^{n} h_i = -\frac{\partial \sigma}{\partial t} \tag{21}$$

Considering the initial conditions given by Eq. (13), the solution of Eq. (21) is given by

$$\sum_{i=1}^{n} h_i = h_0^{\mathrm{s}} - \sigma \tag{22}$$

where

$$h_0^{\mathrm{s}} = \sum_{i=1}^{n} h_{i,0} \tag{23}$$

Substituting Eq. (20) into Eq. (22), it follows that $h_1(\sigma)$. Therefore, Eq. (18) can be rewritten as

$$\frac{\lambda_0}{\lambda(\sigma)} = \left(1 + \frac{\sum_{i=n+1}^{N} h_{i,0} r_{\mathrm{p}i}^4}{\sum_{i=1}^{n} h_i(\sigma) r_{\mathrm{p}i}^4}\right)\left(\frac{\sum_{i=1}^{n} h_{i,0} r_{\mathrm{p}i}^4}{\sum_{i=1}^{N} h_{i,0} r_{\mathrm{p}i}^4}\right) \tag{24}$$

where

$$\lambda_0 = \frac{\sum_{i=1}^{n} h_{i,0} r_{\mathrm{p}i}^4}{\sum_{i=1}^{N} h_{i,0} r_{\mathrm{p}i}^4}\frac{1}{\Delta} \tag{25}$$

Because all h_i (with $i \leq n$) are decreasing functions, from Eq. (24) it follows that λ is also a decreasing function of σ. In addition, DBF occurs only if retention probability tends to zero (Santos and Barros 2010). Therefore,

$$\sum_{i=1}^{n} h_i r_{\mathrm{p}i}^4 << \sum_{i=n+1}^{N} h_i r_{\mathrm{p}i}^4 < \sum_{i=1}^{N} h_i r_{\mathrm{p}i}^4 \tag{26}$$

In this case, Eq. (24) tends to

$$\frac{\lambda(\sigma)}{\lambda_0} = \frac{\sum_{i=1}^{n} h_i(\sigma) r_{\mathrm{p}i}^4}{\sum_{i=1}^{n} h_{i,0} r_{\mathrm{p}i}^4} \tag{27}$$

Assuming that small pores can be represented by an unique pore radii, from Eqs. (27) and (22), it follows that

$$\frac{\lambda(\sigma)}{\lambda_0} = 1 - \frac{\sigma}{h_0^{\mathrm{s}}} \tag{28}$$

References

Alvarez, A.C.: Inverse problems for deep bed filtration in porous media. Ph.D. thesis, IMPA, Rio de Janeiro (2004)

Bradford, S.A., Abriola, L.M.: Dissolution of residual tetrachloroethylene in fractional wettability porous media: incorporation of interfacial area estimates. Water Resour. Res. **37**, 1183–1195 (2001)

Bradford, S.A., Bettahar, M.: Concentration dependent transport of colloids in saturated porous media. J. Contam. Hydrol. **82**, 99–117 (2006)

Bradford, S.A., Yates, S.R., Bettahar, M., Simunek, J.: Physical factors affecting the transport and fate of colloids in saturated porous media. Water Resour. Res. **38**(12), 1327 (2002)

Bradford, S.A., Simunek, J., Bettahar, M., van Genuchten, M.Th., Yates, S.R.: Modeling colloid attachment, straining and exclusion in saturated porous media. Environ. Sci. Technol. **37**, 2242–2250 (2003)

Bradford, S.A., Bettahar, M., Simunek, J., van Genuchten, M.Th.: Straining and attachment of colloids in physically heterogeneous porous media. Vadose Zone J. **3**, 384–394 (2004)

Draper, N.R., Smith, H.: Applied Regression Analysis, 3rd edn. Wiley, New York (1967)

Elimelech, M., Gregory, J., Jia, X., Willians, R.A.: Particle Deposition & Aggregation. Butterworth Heinemann, Portsmouth (1995)

Herzig, J.P., Leclerc, D.M., Le Goff, P.: Flow of suspension through porous media—application to deep bed filtration. Ind. Eng. Chem. **62**(5), 8–35 (1970)

Israelachvili, J.: Intermolecular & Surface Forces. 2nd edn. Elsevier, New York; Academic Press, London (2007)

Ives, K.J., Pienvichitr, V.: Kinetics of the filtration of dilute suspensions. Chem. Eng. Sci. **20**, 965 (1965)

Iwasaki, T.: Some notes on sand filtration. J. Am. Water Works Assoc. **29**, 1591–1602 (1937)

Maroudas, A.: Clarification of suspensions: a study of particle deposition in granular filter media. Ph.D. thesis, University of London, London (1961)

Maroudas, A.: Particle deposition in granular filter media, Pt II. Filtr. Scpar. **8**(2), 115–121 (1966)

Maroudas, A., Eisenklam, P.: Clarification of suspensions: a study of article deposition in granular media. Pt II. A theory of clarification. Chem. Eng. Sci. **20**, 875–888 (1965)

Redman, J.A., Grant, S.B., Olson, T.M., Estes, M.K.: Pathogen filtration, heterogeneity, and the potable reuse of wastewater. Environ. Sci. Technol. **35**, 1798–1805 (2001)

Santos, A., Barros, P.: Multiple particle retention mechanisms during filtration in porous media. Environ. Sci. Technol. **44**, 2515–2521 (2010)

Santos, A., Bedrikovetsky, P.: A stochastic model for particulate suspension flow in porous media. Transp. Porous Med. **62**, 23–53 (2006)

Santos, A., Bedrikovetsky, P., Fontoura, S.: Analytical micro model for size exclusion: pore blocking and permeability reduction. J. Membr. Sci. **308**, 115–127 (2008)

Sharma, M.M., Yortsos, Y.C.: Transport of particulate suspensions in porous media: model formulation. AIChE J. **33**(13), 1636–1643 (1987)

Tien, C., Ramarao, B.V.: Granular Filtration of Aerosols and Hydrosols. Butterworth Heinemann, Portsmouth (1995)

Tufenkji, N., Elimelech, M.: Deviation from classical colloid filtration theory in the presence of repulsive DLVO interactions. Langmuir **20**, 10818–10828 (2004)

Tufenkji, N., Miller, G.F., Harvey, R.W., Elimelech, M.: Transport of cryptosporidium oocysts in porous media: role of straining and physicochemical filtration. Environ. Sci. Technol. **38**, 5932–5938 (2004)

Yao, K., Habibian, M.T., O'Melia, C.R.: Water and wastewater filtration: concepts and applications. Environ. Sci. Technol. **5**(11), 1105–1112 (1971)